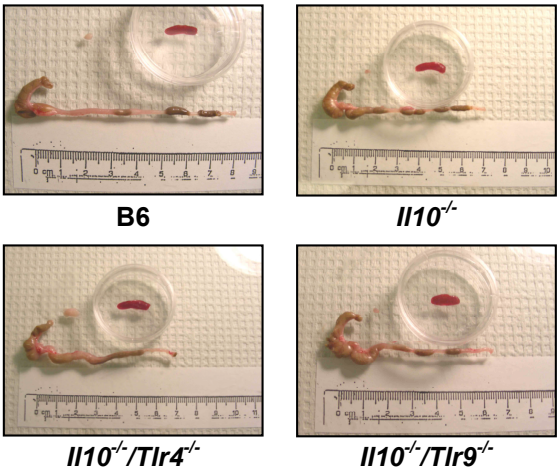

Supplemental Figure 1: Inflammatory profile in *Il10*$^{-/-}$ mutants
Colon, spleen and MLN obtained from B6, *Il10*$^{-/-}$, *Il10*$^{-/-}$/*Tlr4*$^{-/-}$ and *Il10*$^{-/-}$/*Tlr9*$^{-/-}$ mice. Macroscopic signs of intestinal inflammation such as thickening of the intestinal wall and diarrhea were only evident in the colon of *Il10*$^{-/-}$/*Tlr4*$^{-/-}$ mice.

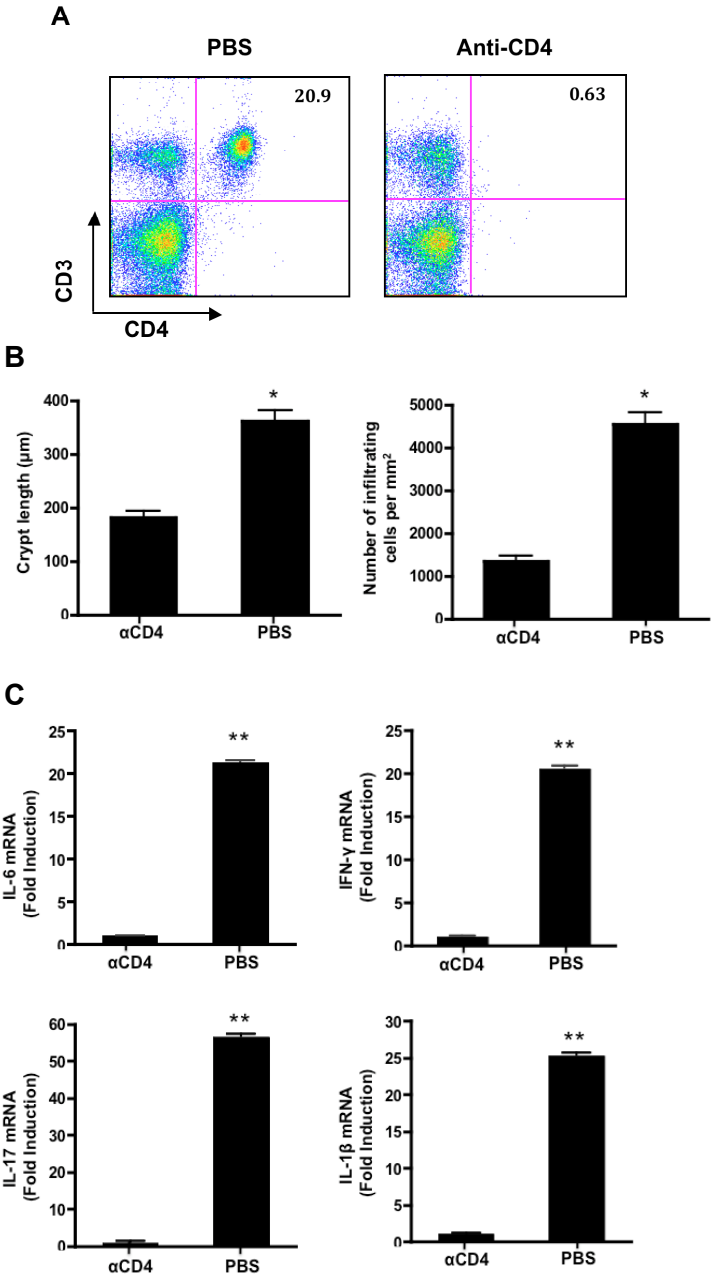

Supplemental Figure 2: CD4 T cell depletion ameliorates intestinal inflammation in *Il10*$^{-/-}$/*Tlr4*$^{-/-}$ mice

(a) CD4+ T cells were depleted, before colitis development, by intraperitoneal (i.p.) administration of 1 mg of anti-CD4 abs (GK1.5, BioExpress) or PBS to 4 weeks old *Il10*$^{-/-}$/*Tlr4*$^{-/-}$ mice. The Flow Cytometry analysis of splenocytes collected 2 weeks after injection confirmed depletion of 97%. **(b)** Evaluation of the H&E stained colon from mice receiving monoclonal anti-CD4 abs (GK1.5) or PBS. CD4 depletion significantly reduced epithelial crypt hyperplasia and cellular infiltration. **(c)** RNA was isolated from colonic homogenates and transcript level of pro-inflammatory cytokines was evaluated by RT-PCR. *Denotes $p<0.05$. **Denotes $p<0.001$.

A

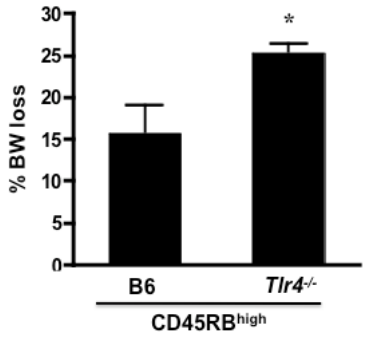

B

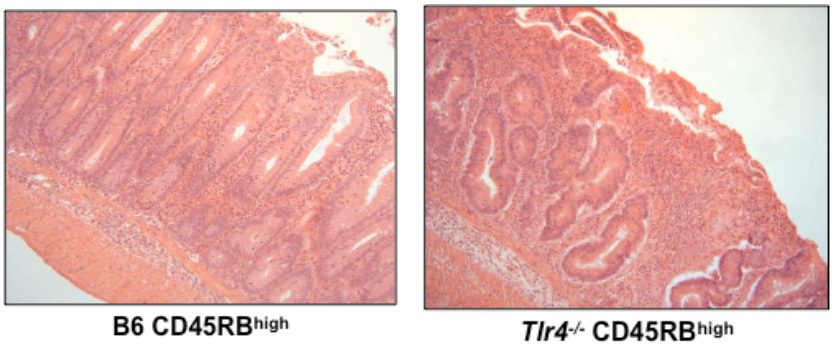

Supplemental Figure 3: Adoptive transfer of naïve *Tlr4*$^{-/-}$ CD4+ T cells induces an aggressive colitis

(a) FACS-sorted CD4+CD45RB^{high} T cells (5x10^5) from B6 (wt) and *Tlr4*$^{-/-}$ mice were adoptively transferred i.p into *Rag1*$^{-/-}$ recipients (n=4 in each group). Mice were monitored weekly for body weight changes and signs of disease. Data reflects increased body weight loss in the mice receiving *Tlr4*$^{-/-}$ naïve T cells seven weeks after transfer. **(b)** Microscopic evaluation of H&E stained colon section revealed more severe inflammatory infiltration, epithelial hyperplasia, dysplasia and crypt abscesses in the colon of *Rag1*$^{-/-}$ mice that had received *Tlr4*$^{-/-}$ naïve T cells. *Denotes $p<0.05$

A

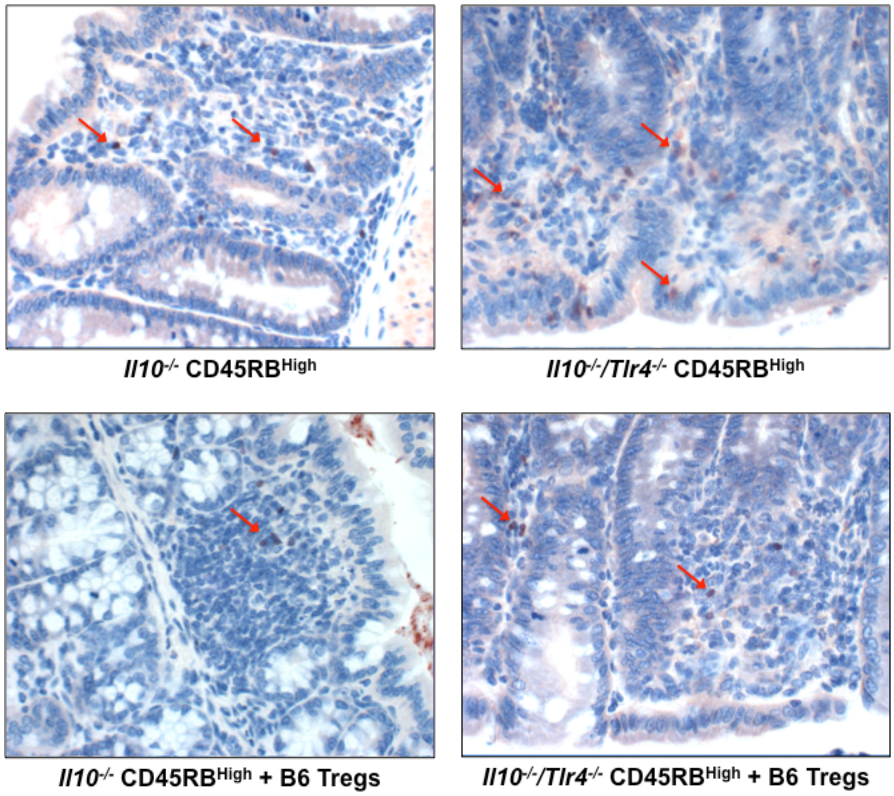

B

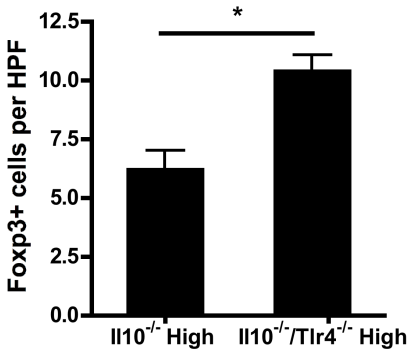

Supplemental Figure 4: Increased Foxp3+ cells in the colons of *Rag1*$^{-/-}$ mice reconstituted with *Il10*$^{-/-}$/*Tlr4*$^{-/-}$ naïve T cells.
(a) Foxp3+ cells in the colons of *Rag1*$^{-/-}$ mice were analyzed by IHC staining of paraffin sections. Rabbit polyclonal antibody to Foxp3 (Abcam) with heat-induced antigen retrieval protocol was used for these stainings. **(b)** Number of Foxp3+ cells counted per high power field (HPF) in two representative pictures of each colon.

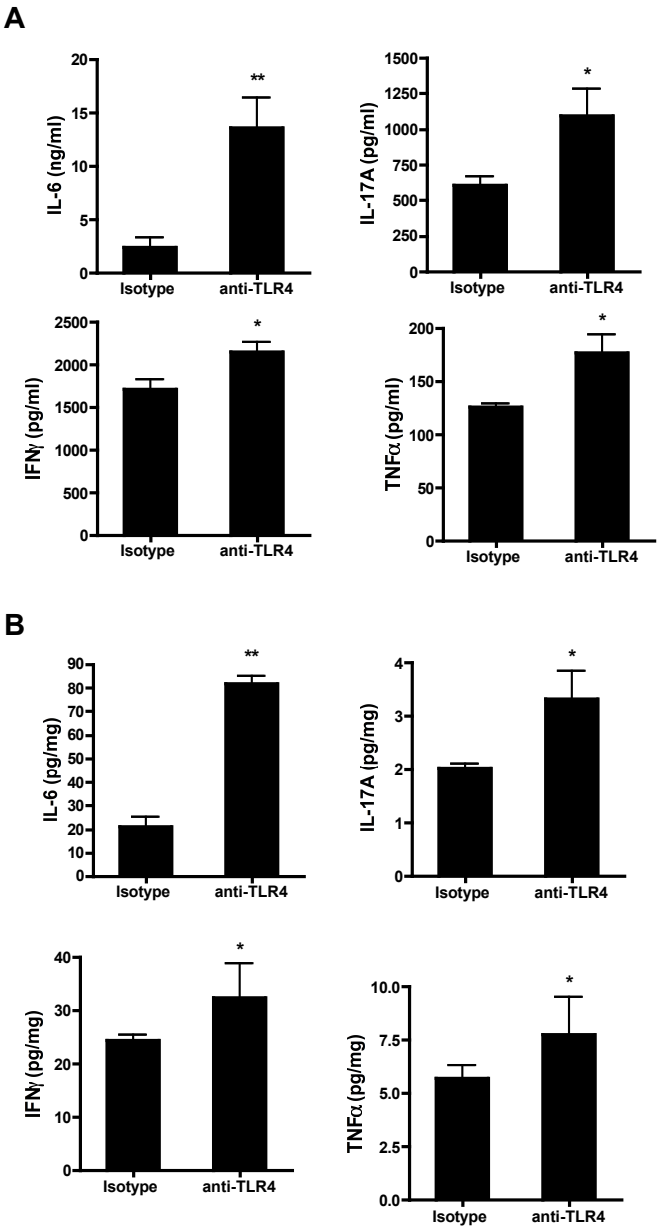

Supplemental Figure 5: In vivo blockade of TLR4 increases the pro-inflammatory profile of *Il10*$^{-/-}$ CD4+ cells.

Blockade of TLR4 in *Il10*$^{-/-}$ mice was carried out by weekly intraperitoneal (i.p.) administration of 100 µg of anti-mouse TLR4/MD2 Ab for two weeks. Rat IgG2a isotype Ab was injected in the control mice under the same conditions. **(a)** Cytokine production by MLN-derived CD4+ cells isolated from *Il10*$^{-/-}$ mice treated with either TLR4 blocking antibody or isotype control, and stimulated with CD3/28 Abs for 24 hours. **(b)** Cytokine levels measured in colonic explants from anti-TLR4 or isotype treated mice, measured after 24 hours of culture.

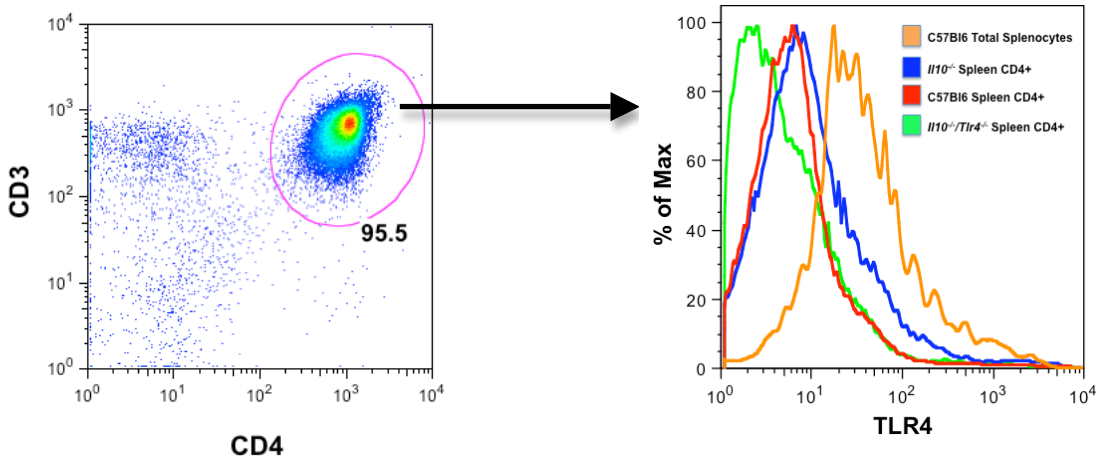

Supplemental Figure 6: TLR4 expression on CD4+ T cells
CD4+ T cells from spleens of *Il10*$^{-/-}$, *Il10*$^{-/-}$*/Tlr4*$^{-/-}$ and B6 mice were purified by immunomagnetic beads isolation using a T cell enrichment kit (Miltenyi Biotec). Cells were then stained with CD3, CD4 and TLR4 (clone MTS510) Abs (all from eBioscience) and analyzed by flow cytometry. TLR4 expression was checked in gated CD3+CD4+ T cells. Data shows expression of TLR4 on *Il10*$^{-/-}$ and B6 T cells (blue and red lines) but not on *Il10*$^{-/-}$*/Tlr4*$^{-/-}$ T cells (green). Total splenocytes from B6 mice were used as a positive control (orange).

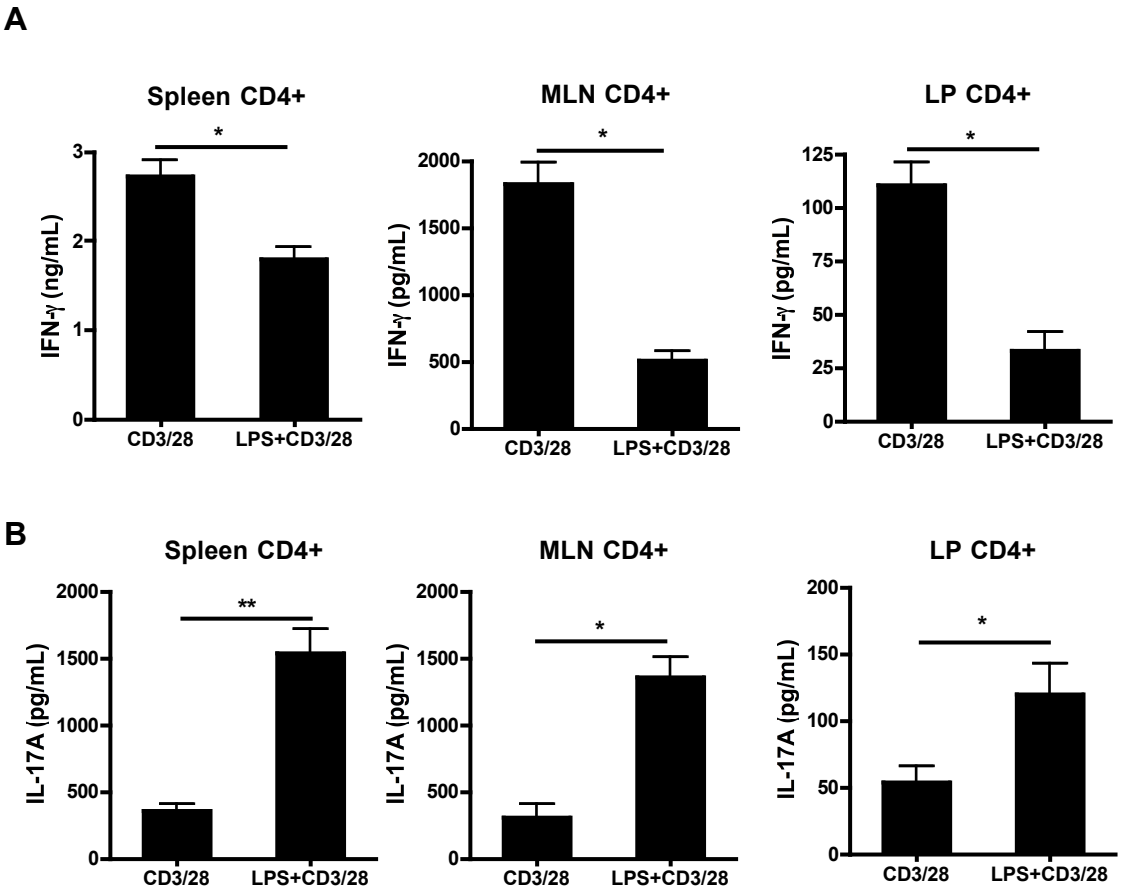

Supplemental Figure 7: LPS pre-stimulation of CD4+ cells from different organs.
(a) IFN-γ production by CD4+ cells isolated from spleen, mesenteric lymph nodes (MLN) and lamina propria (LP) of *Il10*$^{-/-}$ mice. Cells from the different organs were stimulated for 2 hrs with LPS (100ng/mL), or left untreated, before stimulation with anti-CD3 and anti-CD28 Abs. **(b)** IL-17A production by CD4+ cells isolated from the same organs and stimulated as in **a**.
Data (mean ± SD) is representative of two independent experiments. CD4+ T cells from spleen and MLN were purified by FACS sorting (purity >99%). Cells from LP were purified by negative selection using immunomagnetic bead isolation (purity >95%). * denotes $p<0.05$ and ** denotes $p<0.01$

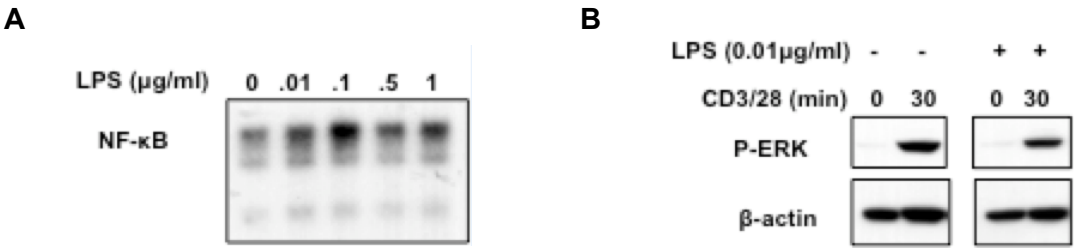

Supplemental Figure 8: Pre-stimulation with sub-optimal doses of LPS controls TCR signaling.
(a) CD4+ T cells were isolated from MLN of *Il10*$^{-/-}$ mice and stimulated with different concentrations of LPS. Two hrs after stimulation, cells were collected and NF-κB nuclear translocation was analyzed by EMSA as described in Methods. As shown, 10-1000 ng/mL of LPS induced NF-κB activation, of which 100 ng/mL provoked the strongest response. **(b)** MLN-derived CD4+ cells from *Il10*$^{-/-}$ mice were isolated and pre-stimulated with 10 ng/mL of LPS or left untreated for 2 hrs. Cells were then stimulated with anti-CD3/28 Abs for the indicated time-points. Pre-stimulation of CD4+ cells with a sub-optimal concentration of LPS (10 ng/mL) also resulted in decreased ERK1/2 phosphorylation after anti-CD3/28 Abs stimulation.

A

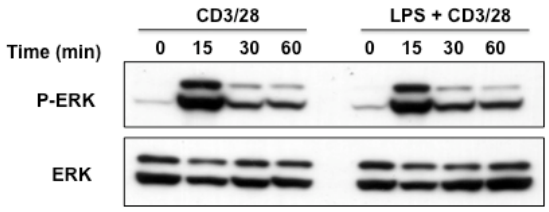

B

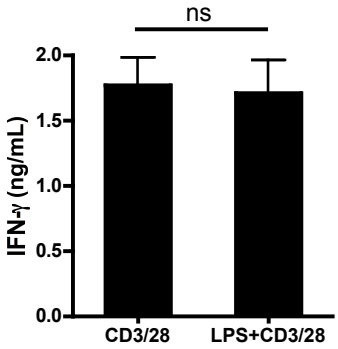

Supplemental Figure 9: Simultaneous stimulation of TLR4 and TCR does not inhibit IFN-γ production or activation of ERK1/2.
Il10$^{-/-}$ MLN-derived CD4+ cells were isolated by FACS-sorting (purity>98%) and co-stimulated simultaneously in vitro with 100 ng/mL of LPS and CD3/28 Abs. **(a)** TCR-dependent phosphorylation of ERK1/2 in the presence or absence of LPS. **(b)** IFN-γ production after 24 hrs of CD3/28 Abs stimulation in the presence or absence of LPS stimulation.

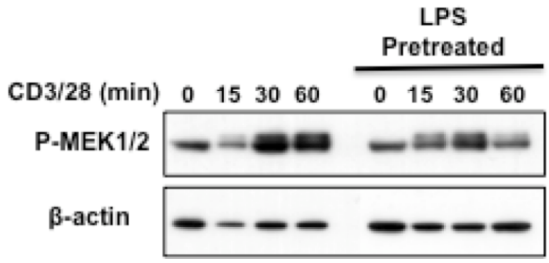

Supplemental Figure 10: LPS pre-treatment does not affect MEK1/2 activation
MLN-derived CD4+ T cells from *Il10*$^{-/-}$ mice were pre-stimulated with 100 ng/mL of LPS or left untreated. Two hrs after LPS pre-treatment, cells were stimulated with anti-CD3/28 Abs for the indicated time-points and the cytosolic protein extracts was subjected to immunoblotting with a Phospho-MEK1/2 specific antibody (Cell Signaling Technologies). LPS pre-treatment did not suppress the TCR-dependent activation of MEK1/2.

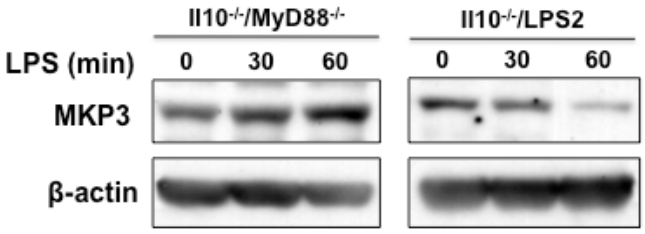

Supplemental Figure 11: MKP-3 activation by LPS is TRIF-dependent.
FACS-sorted MLN-derived CD4+ cells from *Il10*$^{-/-}$*/Myd88*$^{-/-}$ and *Il10*$^{-/-}$*/LPS2*$^{-/-}$ (*Il10*$^{-/-}$*/Trif*$^{-/-}$) mice were isolated and stimulated with 100 ng/mL of LPS for the indicated time points. The purity of the CD4+ T cells was >98%. MKP-3 activation was unaffected by the lack of MyD88 signaling but strongly reduced in the *Il10*$^{-/-}$*/Trif*$^{-/-}$ mice.

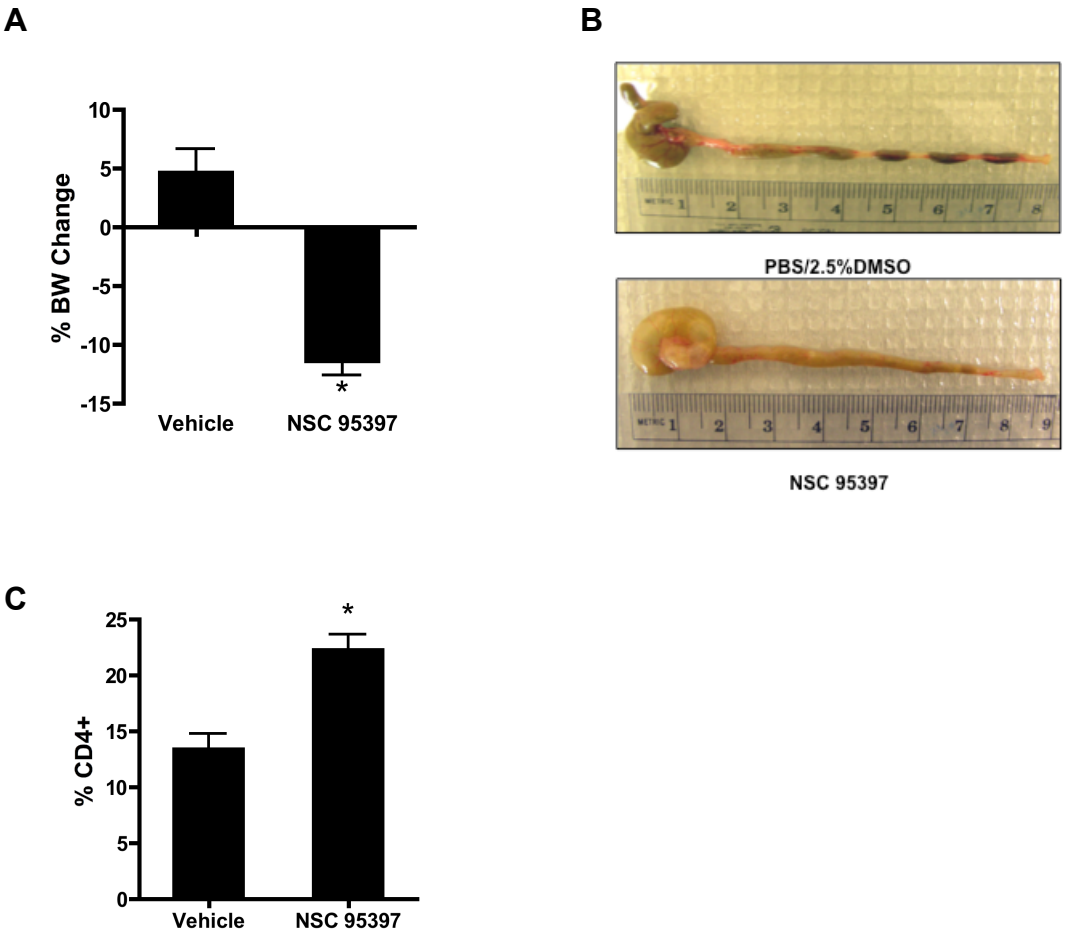

Supplemental Figure 12: Higher inflammatory profile in the mice treated with MKP inhibitor NSC 95397.
(a) Body weight change in *Il10*$^{-/-}$ mice treated with a single dose of the MKP inhibitor NSC 95397 (4mg/Kg of body weight) or vehicle. Data represents body weight change 3 days after the administration of the compound. **(b)** Representative colons of these mice showing signs of intestinal inflammation and diarrhea after NSC 95397 treatment. **(c)** Percentage of CD4+ T cells in the MLN of these two groups of mice.

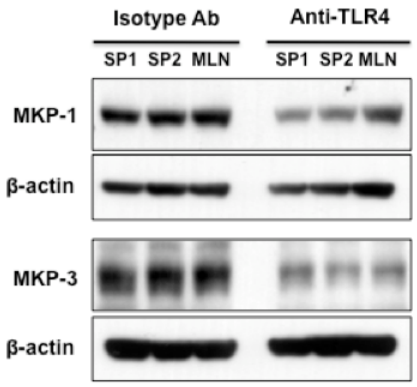

Supplemental Figure 13: Blockade of TLR4 in vivo induces suppression of MKP-1 and -3 expression in CD4+ T cells
In vivo blockade of TLR4 in *Il10*$^{-/-}$ mice was carried out as described in the Methods section. **(a)** CD4+ T cells were isolated from spleen and MLN of these mice and immediately lysed. Protein extracts from the nuclear and cytosolic lysates were then subjected to immunoblot analysis and the levels of MKP-1 and -3 were determined.

	Forward Primer	Reverse Primer
CCL19	5'-ATgTTCAgCAgCCAACTgAg-3'	5'-ACCCTgAgACCATgAggAAg-3'
CCL22	5'-CTATggTgCCAATgTggAAg-3'	5'-TCggTTCTTgACggTTATCA-3'
CD3d	5'-gCCAgAACTgTgTggAgCTA-3'	5'-CTCATgTCCTgCAAAgCAgT-3'
CD4	5'-TCTggCAACCTgACTCTgAC-3'	5'-TCATCACCACCAggTTCACT-3'
CXCL10	5'-gCTgCAACTgCATCCATATC-3'	5'-TTTCATCgTggCAATgATCT-3'
F4/80	5'-TAgTggAggCAgTgATgCTC-3'	5'-TATgACCACCAggACTCCAA-3'
GAPDH	5'-ATCAACgACCCCTTCATTgACC-3'	5'- CCAgTAgACTCCACgAgATACTCAg-3'
IFN-γ	5'-AgCTCTTCCTCATggCTgTT-3'	5'-TTTgCCAgTTCCTCCAgATA-3'
KC	5'-ACCCAAACCgAAgTCATAgC-3'	5'-TTTCTgAACCAAgggAgCTT-3'
IL-12p40	5'-AAACCAgACCCgCCCAAgAAC-3'	5'- AAAAAgCCAACCAAgCAgAAgACAg-3'
IL-17	5'-gCCCTCAgACTACCTCAACC-3'	5'-gAATTCATgTggTggTCCAg-3'
IL-1β	5'-gAAgAAgAgCCCATCCTCTg-3'	5'-TCATCTCggAgCCTgTagTg-3'
IL-23p19	5'-TCCgTTCCAAgATCCTTCg-3'	5'-gAACCTgggCATCCTTAAgC-3'
IL-6	5'-ATCCAgTTgCCTTCTTgggACTgA-3'	5'-AACgCACTAggTTTgCCgAgTAgA-3'
MPO	5'-CCAgCAgCCATgAAgTA-3'	5'-CATAACggAAAgCATTggTg -3'
TLR4	5'-TggCTggTTTACACATCCATCggT-3'	5'-TggCACCATTgAAgCTgAggTCTA -3'
TNF-α	5'-ACAgAAAgCATgATCggCg-3'	5'-gCCCCCCATCTTTTggg -3'

Supplemental Table: Oligonucleotides used for qPCR and conventional PCR analysis.